XLIII CILAMCE
21–25, November, 2022
FOZ DO IGUAÇU – PR – BRAZIL

Numerical observation of traveling wave solution in a non-Newtonian foam model

Jhuan B. Cedro[1], Grigori Chapiro[2].

[1]*Computational Modeling Graduate Program, Federal University of Juiz de Fora*
University campus at José Lourenço Kelmer Street, 36036-900, Minas Gerais, Brazil
jhuancedro@ice.ufjf.br
[2]*Laboratory of Applied Mathematics (LAMAP), Federal University of Juiz de Fora*
University campus at José Lourenço Kelmer Street, 36036-900, Minas Gerais, Brazil
grigori@ice.ufjf.br

Abstract. Foam injection is an oil recovery technique with great potential to be applied in the Brazillian Pre-salt reservoirs. It consists of injecting gas and surfactant solution into the reservoir to control the gas mobility, avoid the fingering formation, and improve sweep efficiency. Investigating the foam flow in porous media is challenging due to foams' non-Newtonian behavior. That is why most mathematical studies on this subject consider Newtonian models. In the literature, there is a non-Newtonian model describing the foam displacement validated through laboratory experiments. In the present work, we numerically verified that this model possesses a traveling wave solution *i.e.,* a stable-shape profile displacing in space with constant velocity. Such a solution is similar to ones appearing in Newtonian models. We validate our results by comparing them to the experimental data found in the literature. The numerical method is based on a finite difference Crank-Nicolson scheme with the Newton-Raphson method for time step evolution.

Keywords: Foam flow in porous media, Traveling waves, Non-Newtonian fluid.

1 Introduction

There is a consistent search for more efficient and less harmful to the environment oil recovery methods. One of these methods consists of controlled injection of water, gas, and surfactant into the reservoir (SAG), leading to the generation of foam, more sweep efficiency, and higher oil recovery factor, Lake et al. [1]. The mentioned technique is also known as foam injection and is an adaptation of the water-alternating-gas (WAG) recovery method.

Mathematical models describe the dynamics of foam flow in porous media through a system of two Partial Differential Equations (PDEs), composed of the Rapoport-Leas equation and a balance law for the foam texture – see Ma et al. [2], Hematpur et al. [3]. There are different approaches for modeling the gas mobility reduction due to the presence of foam. Hirasaki and Lawson [4] proposed a formula describing the foamed gas's apparent viscosity, which depends on the gas velocity, *i.e.*, foam flow has a non-Newtonian behavior. Such behavior makes both analytical and numerical investigation of the foam flow in porous media a challenging task.

Many laboratory experiments yield saturation profiles with the unchanging shape and moving with a constant velocity, see Simjoo et al. [5], Simjoo and Zitha [6], Janssen et al. [7]. This fact motivated many researchers to look for traveling wave solutions for the foam flow models, see Ashoori et al. [8], Lozano et al. [9], Zavala et al. [10], Cedro et al. [11]. However, they assumed that the fluid was Newtonian to find traveling wave solutions analytically.

In this work, we propose to study a non-Newtonian foam model by Chen et al. [12], which uses foamed gas viscosity defined by Hirasaki and Lawson [4]. We show a traveling wave solution using numerical simulations. Once this kind of result is possible to be observed, it can indicate the viability of finding an analytical solution for that foam model.

This paper is structured as follows. In Section 2, we present the foam displacement model, including the non-Newtonian gas viscosity. In Section 3, we describe the numerical scheme used in our simulations. Section 4 shows our numerical experiment configuration, results, and validation with the experimental data. Finally, in Section 4, we summarize our conclusions and discussion.

2 Foam displacement mathematical model

We consider a one-dimensional transient mechanistic foam model composed of two partial differential equations. The first one is the Rapport-Leas equation, a conservation law for the water mass in porous media. The second one is a foam texture balance equation.

$$\begin{cases} \dfrac{\partial}{\partial t}(\phi S_w) + \dfrac{\partial u_w}{\partial x} = 0\,, \\ \dfrac{\partial}{\partial t}(\phi S_g n_D) + \dfrac{\partial}{\partial x}(u_g n_D) = \phi S_g \Phi\,, \end{cases} \tag{1}$$

where ϕ is medium porosity (considered constant), S_w and S_g are the phase saturations, u_w and u_g are the superficial phase velocities – the subscripts w and g denote the aqueous and gaseous phases, respectively. The foam texture n_f is the volumetric bubble density. For simplicity, we adopt the dimensionless variable $n_D = n_f/n_{\max}$, where $n_{\max}$ is a reference value for n_f. We consider a fully saturated medium, *i.e.*, $S_w + S_g = 1$. Finally, Φ describes the bubbles creation and destruction mechanism as detailed in Section 2.1.

The velocities are given by

$$u_w = u f_w + k\lambda_{rg} f_w \frac{\mathrm{d}P_c}{\mathrm{d}x} \qquad \text{with} \qquad u = u_w + u_g\,, \tag{2}$$

where u is the total superficial velocity (assumed to be constant) and P_c is the capillary pressure due to the interaction between different phases with the porous matrix.

Following the standard definitions of fractional flow theory (see Buckley and Leverett [13], Lake [14]), the phase mobilities λ_w and λ_g and the fractional flow functions f_w and f_g are:

$$\lambda_{rw} = \frac{k_{rw}}{\mu_w}\,, \quad \lambda_{rg} = \frac{k_{rg}}{\mu_g} \quad \text{and} \quad \lambda = \lambda_w + \lambda_g\,, \tag{3}$$

$$f_w = \frac{\lambda_w}{\lambda}\,, \quad f_g = \frac{\lambda_g}{\lambda} \quad \Rightarrow\ f_w + f_g = 1\,, \tag{4}$$

where k_{rw} and k_{rg} are the water and gas relative permeabilities, μ_w and μ_g are the phase viscosities, and λ is the total mobility. In the presence of foam, we denote the gas's apparent viscosity as μ_f, as described in Section 2.1.

2.1 Population balance model

In the literature, there are different approaches for modeling the source term Φ, the relative permeability functions k_{rw}, and k_{rg}, the capillary pressure P_c and the foamed gas viscosity μ_f, *e.g.*, Hematpur et al. [3], Ashoori et al. [15], Kovscek et al. [16], Kam and Rossen [17], Thorat and Bruining [18], Zitha [19]. In this work, we adopt the definitions presented by Chen et al. [12].

The relative permeability model is based on Corey [20]:

$$k_{rw} = \begin{cases} 0 & , \quad 0 \le S_w < S_{wc} \\ k^0_{rw}\left(\dfrac{S_w - S_{wc}}{1 - S_{wc}}\right)^{n_w} & , \quad S_{wc} \le S_w \le 1 \end{cases}\,, \tag{5}$$

$$k_{rg} = \begin{cases} k^0_{rg}\left(\dfrac{S_f}{1 - S_{wc}}\right)^{n_g} & , \quad 0 \le S_g \le 1 - S_{wc} \\ 0 & , \quad 1 - S_{wc} < S_g \le 1 \end{cases}\,, \quad S_f = X_f S_g\,, \quad S_g = 1 - S_w\,, \tag{6}$$

where S_{wc} is the residual water saturation, and k^0_{rw}, k^0_{rg}, n_w, n_g are the model's parameters. We assume there is a fraction X_t of the gaseous phase, which is immobile in the porous medium, while only the gaseous fraction X_f flows (Kovscek et al. [16]). Then we denote S_f as the flowing gas saturation. That trapped gas fraction is described as:

$$X_t = X_{t,\max}\left(\frac{\beta n_t}{1 + \beta n_t}\right)\,, \qquad X_t + X_f = 1\,, \quad n_t \approx n_f\,, \tag{7}$$

where $X_{t,\max}$ is the maximum trapped foam fraction, β is a trapping parameter, and n_t is the trapped foam texture. The capillary pressure function follows the model proposed by Leverett [21], with parameters fitted to experiments

of Kovscek et al. [16]:

$$P_c = \sigma_{wg}\sqrt{\frac{\phi}{k}}\left(\frac{0.022}{S_w - 0.15}\right)^{0.2}, \tag{8}$$

where σ_{wg} is the interfacial tension between water and gas. The foamed gas apparent viscosity is given by Hirasaki and Lawson [4]:

$$\mu_f = \mu_g^0 + \alpha\frac{n_f}{v_g^{1/3}} \quad \text{with} \quad v_g = \frac{u_g}{\phi S_g}, \tag{9}$$

where μ_g^0 is the gas viscosity in the absence of foam, and v_g is the gas interstitial velocity. That expression model a non-Newtonian shear-thinning foam's behavior once its viscosity decreases with increasing velocity. Finally, the source term Φ is defined as:

$$\begin{gathered}\Phi = r_g - r_c, \\ r_g = k_1^0(1 - n_D^\omega)v_w v_g^{\frac{1}{3}}, \qquad r_c = k_{-1}^0\left(\frac{P_c}{P_c^* - P_c}\right)^2 v_g n_f, \qquad \omega = 3,\end{gathered} \tag{10}$$

where k_1^0 and k_{-1}^0 are constants, and P_c^* is the limiting capillary pressure, above which foam abruptly coalesces. In Chen et al. [12], Kovscek et al. [16] the authors consider P_c^* depending on the surfactant concentration C_s. This work considers that surfactant concentration is far above the critical micelle concentration. In this case, there is enough surfactant for foam generation and stability, yielding small C_s variations that do not affect the foam behavior, see Kile and Chiou [22]. Therefore, we consider P_c^* is constant.

3 Numerical scheme

This section presents details of the numerical simulation for the system (1). We employ a Reaction-Convection-Diffusion simulator (RCD) (see Lambert et al. [23] for details), which implements a finite difference scheme for solving the following system of equations:

$$\frac{\partial}{\partial t}G(U) + \frac{\partial}{\partial x}F(U) = \frac{\partial}{\partial x}\left(B(U)\frac{\partial U}{\partial x}\right) + R(U), \tag{11}$$

where U represents the problem variables. The functions G, F, B and R have the following discretization schemes:

$$\frac{\partial}{\partial t}G(U) \approx \frac{G_m^{n+1} - G_m^n}{\Delta t}, \tag{12}$$

$$\frac{\partial}{\partial x}F(U) \approx \alpha\frac{F_{m+1}^{n+1} - F_{m-1}^{n+1}}{2\Delta x} + (1-\alpha)\frac{F_{m+1}^n - F_{m-1}^n}{2\Delta x}, \tag{13}$$

$$\begin{aligned}\frac{\partial}{\partial x}\left(B(U)\frac{\partial U}{\partial x}\right) \approx \quad & \alpha\frac{(B_{m+1}^{n+1} + B_m^{n+1})(U_{m+1}^{n+1} - U_m^{n+1}) - (B_m^{n+1} + B_{m-1}^{n+1})(U_m^{n+1} - U_{m-1}^{n+1})}{2(\Delta x)^2} \\ & +(1-\alpha)\frac{(B_{m+1}^n + B_m^n)(U_{m+1}^n - U_m^n) - (B_m^n + B_{m-1}^n)(U_m^n - U_{m-1}^n)}{2(\Delta x)^2}\end{aligned}, \tag{14}$$

$$R \approx \alpha R_m^{n+1} + (1-\alpha)R_m^n, \tag{15}$$

where m and n denote the spatial and temporal discretizations, respectively, and Δx and Δt are spatial and temporal step sizes. Notice that, temporal discretization is fully implicit for $\alpha = 1$ and explicit for $\alpha = 0$. In this work, we adopt $\alpha = 1/2$, also known as Crank and Nicolson [24] scheme (see LeVeque [25]).

By replacing (12)-(15) in (11), and grouping implicit and explicit terms in $\mathbb{F}$ and $\mathbb{Y}$, we obtain:

$$\underbrace{\frac{G_m^{n+1}}{\Delta t} + \frac{\alpha}{2\Delta x}(F_{m+1}^{n+1} - F_{m-1}^{n+1})}_{\mathbb{F}_m(U_{m-1}^{n+1}, U_m^{n+1}, U_{m+1}^{n+1})} = \underbrace{\frac{G_m^n}{\Delta t} + \frac{\alpha - 1}{2\Delta x}(F_{m+1}^n - F_{m-1}^n)}_{\mathbb{Y}_m(U^n)}. \tag{16}$$

For each meshpoint m, we define:

$$\mathbb{G}_m = \mathbb{F}_m - \mathbb{Y}_m = 0 \tag{17}$$

and numerically find the solution of the global system $\mathbb{G}(U^{n+1}) = 0$. Since G, F, B e R are non-linear functions, the roots of $\mathbb{G}$ are obtained through the Newton–Raphson method.

For the foam flow, substituting eqs. (2)-(4) into the system (1) and considering that the velocity u and porosity ϕ are constants, we rewrite system (1) as:

$$\begin{cases} \dfrac{\partial S_w}{\partial t} + \dfrac{u}{\phi}\dfrac{\partial f_w}{\partial x} = -\dfrac{k}{\phi}\dfrac{\partial}{\partial x}\left(\left(f_w \dfrac{k_{rg}}{\mu_g}\dfrac{\mathrm{d}P_c}{\mathrm{d}S_w}\right)\dfrac{\partial S_w}{\partial x}\right), \\ \dfrac{\partial}{\partial t}(S_g n_D) + \dfrac{u}{\phi}\dfrac{\partial}{\partial x}(f_g n_D) = \dfrac{k}{\phi}\dfrac{\partial}{\partial x}\left(\left(f_w \dfrac{k_{rg}}{\mu_g}\dfrac{dP_c}{dS_w} n_D\right)\dfrac{\partial S_w}{\partial x}\right) + S_g\Phi\,. \end{cases} \tag{18}$$

This system fits the general form give in eq. (11) with the following matrices:

$$U = \begin{bmatrix} S_w \\ n_D \end{bmatrix}, \quad G(U) = \begin{bmatrix} S_w \\ S_g n_D \end{bmatrix}, \quad F(U) = \frac{u}{\phi}\begin{bmatrix} f_w \\ f_g n_D \end{bmatrix}, \quad R(U) = \begin{bmatrix} 0 \\ S_g\Phi \end{bmatrix}, \tag{19}$$

$$B(U) = \frac{k}{\phi}\begin{bmatrix} -f_w \dfrac{k_{rg}}{\mu_g}\dfrac{\mathrm{d}P_c}{\mathrm{d}S_w} + \epsilon_{S_w} & 0 \\ f_w \dfrac{k_{rg}}{\mu_g}\dfrac{\mathrm{d}P_c}{\mathrm{d}S_w} n_D & \epsilon_{n_D} \end{bmatrix}. \tag{20}$$

We need to deal with the implicit dependence between apparent foam viscosity μ_f and the gas velocity v_g in eq. (9). One can replace relations from eqs. (2)-(4) in eq. (9) to obtain a cubic expression of μ_f and explicitly write μ_f as function of S_w, n_D and $\mathrm{d}P_c/\mathrm{d}x$ – see Pereira and Chapiro [26]. In the numerical simulation, we kept that single derivative one step behind in time, so the model still fits the general form of eq. (11).

3.1 Boundary and initial conditions

Furthermore, we adopt a Dirichlet boundary condition on the left side to simulate a fixed saturation injection value and a homogeneous Neumann condition on the right side to simulate an infinite domain outlet condition. The initial solution is set as the following Riemann Problem:

$$U = (S_w, n_D) = \begin{cases} (S_w^-, n_D^-)\,, & x \le 0 \\ (S_w^+, n_D^+)\,, & x > 0 \end{cases}. \tag{21}$$

These boundary and initial condition were used as they help identifying traveling wave profiles, see Lozano et al. [9], Zavala et al. [10], Lozano et al. [27] for details.

In order to match the experimental data from Chen et al. [12], we need the initial conditions in (21). The values S_w^- and S_w^+ were estimated from the reported experimental observations in Chen et al. [12]. As proved for other models, the boundary conditions for the stable traveling wave solution need to satisfy local equilibrium conditions, as described by Ashoori et al. [8], Lozano et al. [9], Zavala et al. [10], Cedro et al. [11], *i.e.* the source term $\Phi = 0$ at (S_w^-, n_D^-) and at (S_w^+, n_D^+). Substituting these boundary conditions into (10), we obtain:

$$k_1^0(1-(n_D^\pm)^3)v_w(S_w^\pm, n_D^\pm)v_g(S_w^\pm, n_D^\pm)^{\frac{1}{3}} - k_{-1}^0\left(\frac{P_c(S_w^\pm)}{P_c^* - P_c(S_w^\pm)}\right)^2 v_g(S_w^\pm, n_D^\pm)n_D^\pm n_{\max} = 0\,. \tag{22}$$

From the physical point of view, the local equilibrium condition means the situation when the foam creation rate coincides with the foam coalescence. We solved (22) numerically to obtain the values of n_D^+ and n_D^-.

4 Matching laboratory experiment

In this section, we numerically reproduce the experiments reported by Chen et al. [12] and show the existence of a traveling wave solution for the model proposed by the authors. We consider a model by Chen et al. [12] with the same parameter values, except for S_{wc} and P_c^*, (see Table 1). The only parameter we set different from Chen et al. [12] was the connate water saturation S_{wc} value. We observe that the connate water saturation S_{wc} significantly affects the wavefront velocity. Considering the adversity in obtaining residual saturations in the core-flood porous media experiments, we set the S_{wc} value that better fits the experimental average wavefront velocity,

Table 1. Model parameters for foam flow simulation.

Two-phase flow		Population balance	
Parameter	Value	Parameter	Value
k	$3 \cdot 10^{-13}\,\mathrm{m}^2$	k_1^0	$1.5 \cdot 10^{15}\ \mathrm{s}^{\frac{1}{3}}\,\mathrm{m}^{\frac{13}{3}}$
ϕ	0.18	k_{-1}^0	$10\,\mathrm{m}^{-1}$
n_w	3	P_c^*	$3 \cdot 10^4\,\mathrm{Pa}$
k_{rw}^0	0.7	α	$7.4 \cdot 10^{-18}\ \mathrm{Pa}\,\mathrm{s}^{\frac{2}{3}}\,\mathrm{m}^{\frac{10}{3}}$
n_g	3	$X_{t,\max}$	0.78
k_{rg}^0	1.0	$n_{\max}$	$10^{12}\,\mathrm{m}^{-13}$
S_{wc}	0.2797		
μ_w	$1.0 \cdot 10^{-3}\,\mathrm{Pa} \cdot \mathrm{s}$		
μ_g	$1.8 \cdot 10^{-5}\,\mathrm{Pa} \cdot \mathrm{s}$		

$S_{wc} = 0.2797$. The constant value of P_c^* is estimated from Kovscek et al. [16] for high values of surfactant concentration.

The values of S_w^- and S_w^+ were estimated from experimental observations reported by Chen et al. [12]. The values of n_D^- and n_D^+ were calculated using eq. (22):

$$\begin{aligned}(S_w^-, n_D^-) &= (0.541245,\ 0.82495200)\,,\\ (S_w^+, n_D^+) &= (0.999000,\ 0.99999697)\,.\end{aligned} \tag{23}$$

Figure 1 presents our numerical results together with the experimental data from Chen et al. [12]. As one can observe, the simulated saturation curves present a shock-like profile that does not change shape over time, with boundary conditions defined by the constant values S_w^-, and S_w^+. There is a good match between numerical and experimental data; however, the experimental results present a smoother water saturation profile. The location of both wavefronts is close to each other, indicating they have similar wave velocities. The wavefront velocity of the numerical simulation is estimated using the space position of the water saturation profile at the fixed value $S_w = 0.8$ (gray dashed line in Fig. 1); the average wavefront velocity is $v = 1.442501 \times 10^{-4}\,\mathrm{m/s}$.

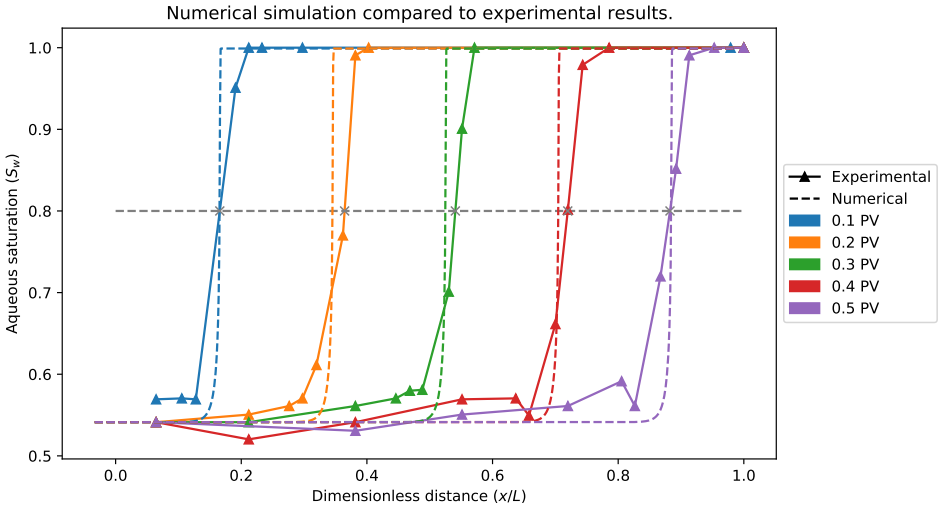

Figure 1. Experimental water saturation profiles from Chen et al. [12] compared to numerical simulations. The dashed gray line stands for the height $S_w = 0.8$ at which experimental wavefront velocity is calculated.

To measure the distance between the numerical solution and experimental results, we use a mean percentage squared error (MPSE) defined as:

$$\mathrm{MPSE} = \sqrt{\frac{1}{L}\int_0^L \left(\frac{\tilde{S_w}(x) - p_1(x)}{p_1(x)}\right)^2 \mathrm{d}x}\,, \qquad p_1(x) \approx S_w(x)\,, \tag{24}$$

where $\tilde{S_w}$ is the numerical solution and p_1 is the linear interpolation of experimental water saturation S_w. Figure 2 shows that MPSE's most significant values are close to the wavefront. Notice that the maximum relative error is approximately 6% and tends to stabilize over time, *i.e.*, the simulated and experimental profiles approach each other over time.

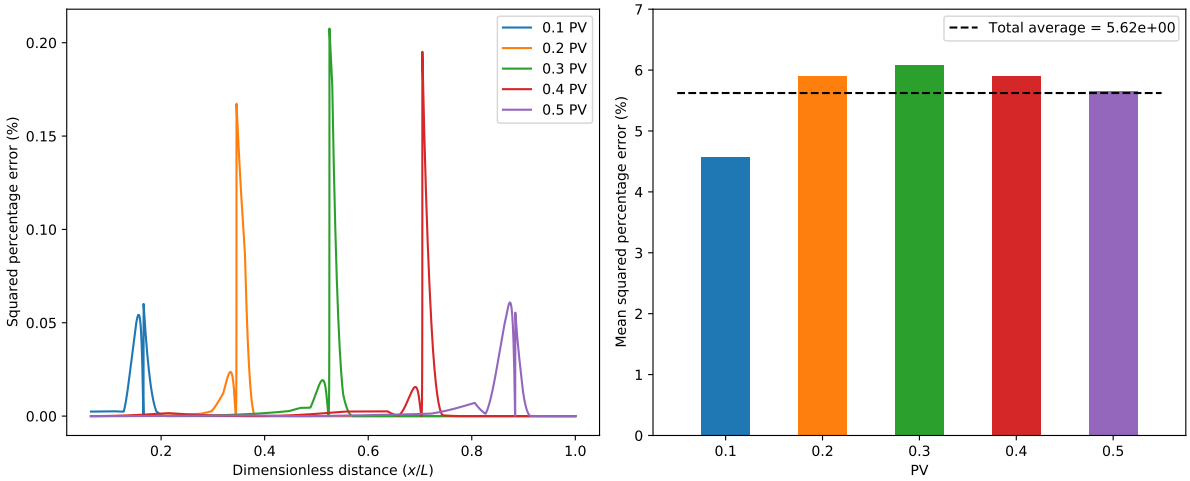

Figure 2. Percentage squared errors between numerical results and experimental data for water saturatio.

5 Conclusions

In this work, we numerically investigate the existence of traveling wave solutions in a non-Newtonian foam model. We obtained a numerical simulation for that model, and the results are in good agreement with experimental data. In particular, the simulated wavefront velocity coincides with the experimental one. The simulation results indicate the existence of a traveling wave solution for the studied model. These results may encourage the search for analytical solutions in the form of traveling waves for non-Newtonian models describing the foam flow in porous media.

Acknowledgements. The current work was conducted in association with the R&D projects ANP n° 20715-9, "Modelagem matemática e computacional de injeção de espuma usada em recuperação avançada de petróleo" (UFJF/Shell Brazil/ANP). Shell Brazil funds it in accordance with ANP's R&D regulations under the Research, Development, and Innovation Investment Commitment. This project is carried out in partnership with Petrobras.

G. Chapiro was supported in part by CNPq grants 303245/2019-0 and 405366/2021-3, and FAPEMIG grant APQ-00405-21.

Authorship statement. The authors hereby confirm that they are the sole liable persons responsible for the authorship of this work, and that all material that has been herein included as part of the present paper is either the property (and authorship) of the authors, or has the permission of the owners to be included here.

References

[1] L. W. Lake, R. Johns, W. R. Rossen, and G. Pope. *Fundamentals of Enhanced Oil Recovery*. Society of Petroleum Engineers, 2014.

[2] K. Ma, G. Ren, K. Mateen, D. Morel, and P. Cordelier. Modeling techniques for foam flow in porous media. *SPE Journal*, vol. 20, n. 3, pp. 453–470, 2015.

[3] H. Hematpur, S. M. Mahmood, N. H. Nasr, and K. A. Elraies. Foam flow in porous media: Concepts, models and challenges. *Journal of Natural Gas Science and Engineering*, vol. 53, pp. 163–180, 2018.

[4] G. J. Hirasaki and J. B. Lawson. Mechanisms of foam flow in porous media: apparent viscosity in smooth capillaries. *SPE Journal*, vol. 25, n. 02, pp. 176–190, 1985.

[5] M. Simjoo, Y. Dong, A. Andrianov, M. Talanana, and P. L. J. Zitha. Novel insight into foam mobility control. *SPE Journal*, vol. 18, n. 3, 2013.

[6] M. Simjoo and P. L. J. Zitha. Modeling of foam flow using stochastic bubble population model and experimental validation. *Transport in Porous Media*, vol. 107, n. 3, pp. 799–820, 2015.
[7] M. T. G. Janssen, F. A. Torres Mendez, and P. L. J. Zitha. Mechanistic modeling of water-alternating-gas injection and foam-assisted chemical flooding for enhanced oil recovery. *Industrial & Engineering Chemistry Research*, vol. 59, n. 8, pp. 3606–3616, 2020.
[8] E. Ashoori, D. Marchesin, and W. R. Rossen. Roles of transient and local equilibrium foam behavior in porous media: traveling wave. *Colloids and Surfaces A: Physicochemical and Engineering Aspects*, vol. 377, pp. 228–242, 2011a.
[9] L. F. Lozano, R. Q. Zavala, and G. Chapiro. Mathematical properties of the foam flow in porous media. *Computational Geosciences*, vol. 25, n. 1, pp. 515–527, 2021.
[10] R. Q. Zavala, L. F. Lozano, P. L. J. Zitha, and G. Chapiro. Analytical solution for the population-balance model describing foam displacement. *Transport in Porous Media*, vol. , 2021.
[11] J. B. Cedro, R. V. Quispe, M. C. Coaquira, L. F. Lozano, and G. Chapiro. Estudo de um modelo cinético para escoamento de espuma em meios porosos. In *XL Ibero-Latin-American Congress on Computational Methods in Engineering (CILAMCE)*, Natal, Brazil, 2019.
[12] Q. Chen, M. G. Gerritsen, and A. R. Kovscek. Modeling foam displacement with the local-equilibrium approximation: theory and experimental verification. *SPE Journal*, vol. 15, n. 01, pp. 171–183, 2010.
[13] S. E. Buckley and M. C. Leverett. Mechanism of fluid displacement in sands. *Transactions of the AIME*, vol. 146, 1942.
[14] L. Lake. *Enhanced oil recovery*. Prentice Hall, New Jersey, 1989.
[15] E. Ashoori, D. Marchesin, and W. R. Rossen. Dynamic foam behavior in the entrance region of a porous medium. *Colloids and Surfaces A: Physicochemical and Engineering Aspects*, vol. 377, pp. 217–227, 2011b.
[16] A. R. Kovscek, T. W. Patzek, and C. J. Radke. A mechanistic population balance model for transient and steady-state foam flow in Boise sandstone. *Chemical Engineering Science*, vol. 50, n. 23, pp. 3783–3799, 1995.
[17] S. I. Kam and W. R. Rossen. A model for foam generation in homogeneous media. *SPE Journal*, vol. 8, n. 4, pp. 417–425, 2003.
[18] R. Thorat and H. Bruining. Foam flow experiments. I. Estimation of the bubble generation-coalescence function. *Transport in Porous Media*, vol. 112, n. 1, pp. 53–76, 2016.
[19] P. L. J. Zitha. A new stochastic bubble population model for foam in porous media. In *SPE/DOE Symposium on Improved Oil Recovery*. Society of Petroleum Engineers, 2006.
[20] A. T. Corey. The interrelation between gas and oil relative permeabilities. *Producers monthly*, vol. 19, n. 1, pp. 38–41, 1954.
[21] M. C. Leverett. Capillary behavior in porous solids. *Trans. AIME*, vol. 142, n. 01, pp. 152–169, 1941.
[22] D. E. Kile and C. T. Chiou. Water solubility enhancements of DDT and trichlorobenzene by some surfactants below and above the critical micelle concentration. *Environmental Science & Technology*, vol. 23, n. 7, pp. 832–838, 1989.
[23] W. Lambert, A. Alvarez, I. Ledoino, D. Tadeu, D. Marchesin, and J. Bruining. Mathematics and numerics for balance partial differential-algebraic equations (PDAEs). *Journal of Scientific Computing*, vol. 84, n. 2, pp. 1–56, 2020.
[24] J. Crank and P. Nicolson. A practical method for numerical evaluation of solutions of partial differential equations of the heat-conduction type. *Mathematical Proceedings of the Cambridge Philosophical Society*, vol. 43, pp. 50–67, 1947.
[25] R. J. LeVeque. *Finite volume methods for hyperbolic problems*. Cambridge University Press, 2002.
[26] W. S. Pereira and G. Chapiro. Mathematical comparison of Newtonian and non-Newtonian foam flow models in porous media. *In preparation*, vol. , 2022.
[27] L. F. Lozano, J. B. Cedro, R. Q. Zavala, and G. Chapiro. How simplifying capillary effects can affect the traveling wave solution profiles of the foam flow in porous media. *International Journal of Non-Linear Mechanics*, vol. 139, pp. 103867, 2022.